Cite as: T. N. Starr *et al.*, *Science* 10.1126/science.abf9302 (2021).

Prospective mapping of viral mutations that escape antibodies used to treat COVID-19

Tyler N. Starr[1]*, Allison J. Greaney[1,2,3]*, Amin Addetia[1,4], William W. Hannon[1,4], Manish C. Choudhary[5], Adam S. Dingens[1], Jonathan Z. Li[5], Jesse D. Bloom[1,2,6]†

[1]Basic Sciences and Computational Biology, Fred Hutchinson Cancer Research Center, Seattle, WA 98109, USA. [2]Department of Genome Sciences, University of Washington, Seattle, WA 98109, USA. [3]Medical Scientist Training Program, University of Washington, Seattle, WA 98109, USA. [4]Molecular and Cellular Biology Graduate Program, University of Washington, Seattle, WA 98109, USA. [5]Brigham and Women's Hospital, Harvard Medical School, Boston, MA 02115, USA. [6]Howard Hughes Medical Institute, Seattle, WA 98109, USA.

*These authors contributed equally to this work.

†Corresponding author. Email: jbloom@fredhutch.org

Antibodies are a potential therapy for SARS-CoV-2, but the risk of the virus evolving to escape them remains unclear. Here we map how all mutations to SARS-CoV-2's receptor-binding domain (RBD) affect binding by the antibodies in the REGN-COV2 cocktail and the antibody LY-CoV016. These complete maps uncover a single amino-acid mutation that fully escapes the REGN-COV2 cocktail, which consists of two antibodies targeting distinct structural epitopes. The maps also identify viral mutations that are selected in a persistently infected patient treated with REGN-COV2, as well as during in vitro viral escape selections. Finally, the maps reveal that mutations escaping the individual antibodies are already present in circulating SARS-CoV-2 strains. Overall, these complete escape maps enable interpretation of the consequences of mutations observed during viral surveillance.

Antibodies are being developed as therapeutics to combat SARS-CoV-2 (*1*). Antibodies against some other viruses can be rendered ineffective by viral mutations that are selected during treatment of infected patients (*2*, *3*) or that spread globally to confer resistance on entire viral clades (*4*). Therefore, determining which SARS-CoV-2 mutations escape key antibodies is essential for assessing how mutations observed during viral surveillance may impact the efficacy of antibody treatments.

Most leading anti-SARS-CoV-2 antibodies target the viral receptor-binding domain (RBD), which mediates binding to the ACE2 receptor (*5*, *6*). We recently developed a deep mutational scanning method to map how all mutations to the RBD affect its function and recognition by antiviral antibodies (*7*, *8*). This method involves creating libraries of RBD mutants, expressing them on the surface of yeast, and using fluorescence-activated cell sorting and deep sequencing to quantify how each mutation affects RBD folding, ACE2 affinity (measured across a titration series), and antibody binding (fig. S1A). Here we used the duplicate mutant libraries described in (*7*), which consist of barcoded RBD variants that cover 3804 of the 3819 possible amino acid mutations. Our libraries were made in the context of the RBD from the early isolate Wuhan-Hu-1, which still represents the most common RBD sequence although several mutants are currently increasing in frequency (*9*, *10*). We mapped how the 2034 mutations that do not strongly disrupt RBD folding and ACE binding (*7*) affected binding by recombinant forms of the two antibodies in Regeneron's REGN-COV2 cocktail (REGN10933 and REGN10987) (*11*, *12*), and Eli Lilly's LY-CoV016 antibody (also known as CB6 or JS016) (*13*) (fig. S1B). REGN-COV2 was recently granted an emergency use authorization for treatment of COVID-19 (*14*), while LY-CoV016 is currently in phase 3 clinical trials (*15*).

We completely mapped RBD mutations that escape binding by the three individual antibodies as well as the REGN10933 + REGN10987 cocktail (Fig. 1, A and B, and zoomable maps at https://jbloomlab.github.io/SARS-CoV-2-RBD_MAP_clinical_Abs/). REGN10933 and REGN10987 are escaped by largely nonoverlapping sets of mutations in the RBD's receptor-binding motif (Fig. 1A), consistent with structural work showing that these antibodies target distinct epitopes in this motif (*11*). But surprisingly, one mutation (E406W) strongly escapes the cocktail of both antibodies (Fig. 1A). The escape map for LY-CoV016 also reveals escape mutations at a number of different sites in the RBD (Fig. 1B). Although some escape mutations impair the RBD's ability to bind ACE2 or be expressed in properly folded form, many come at little or no cost to these functional properties according to prior deep mutational scanning measurements using yeast-displayed RBD (*7*) (color gradient in Fig. 1, A and B, indicates loss of ACE2 affinity and in fig. S2 indicates decrease in RBD expression).

To validate the antigenic effects of key mutations, we

performed neutralization assays using spike-pseudotyped lentiviral particles, and found concordance between the antibody-binding escape maps and neutralization assays (Fig. 1C and fig. S3). As expected from the maps for the REGN-COV2 antibodies, a mutation at site 486 escaped neutralization only by REGN10933, whereas mutations at sites 439 and 444 escaped neutralization only by REGN10987—and so none of these mutations escaped the cocktail. But E406W escaped both individual REGN-COV2 antibodies, and thus also strongly escaped the cocktail. Structural analyses and viral-escape selections led Regeneron to posit that no single amino-acid mutation could escape both antibodies in the cocktail (*11*, *12*), but our complete maps identify E406W as a cocktail escape mutation. Importantly, E406W impacts the REGN-COV2 antibodies in a relatively specific way and does not grossly perturb the function of the RBD, since it only mildly reduces neutralization by LY-CoV016 (Fig. 1C) and the titers of spike-pseudotyped lentiviral particles (fig. S3F).

To explore if our escape maps are consistent with how the virus evolves under antibody selection, we first examined data from Regeneron's viral escape-selection experiments in which spike-expressing VSV was grown in cell culture in the presence of REGN10933, REGN10987, or the cocktail (*12*). That work identified five escape mutations from REGN10933, two from REGN10987, and none from the cocktail (Fig. 2A). All seven cell-culture-selected mutations were prominent in our escape maps while also being accessible by just a single-nucleotide change to the wildtype codon in the Wuhan-Hu-1 RBD sequence (Fig. 2B), demonstrating concordance between the escape maps and viral evolution under antibody pressure in cell culture. Notably, E406W is not accessible by a single-nucleotide change, which may explain why it was not identified by the Regeneron cocktail selections despite being relatively well tolerated for RBD folding and ACE2 affinity.

To determine if the escape maps could inform analysis of viral evolution in infected humans, we examined deep sequencing data from a persistently infected immunocompromised patient who was treated with REGN-COV2 at day 145 after diagnosis with COVID-19 (*16*). The late timing of treatment allowed ample time for the patient's viral population to accumulate genetic diversity, some of which could have been driven by immune pressure since the patient mounted a weak autologous neutralizing antibody response prior to treatment (*16*). Administration of REGN-COV2 was followed by rapid changes in the frequencies of five amino-acid mutations in the RBD (Fig. 2C and fig. S4). Our escape maps showed that three of these mutations escaped REGN10933, and one escaped REGN10987 (Fig. 2B). Notably, the mutations did not all sweep to fixation after antibody treatment: instead, there were competing rises and falls (Fig. 2C). This pattern has been observed in the adaptive within-host evolution of other viruses (*17*, *18*), and can arise from genetic hitchhiking and competition among viral lineages. Both these forces appear to be at play in the persistently infected patient (Fig. 2C and fig. S4C): E484A (not an escape mutation in our maps) hitchhikes with F486I (which escapes REGN10933) after treatment, and the viral lineage carrying N440D and Q493K (which escape REGN10987 and REGN10933, respectively) competes first with the REGN10933 escape-mutant Y489H, and then with the E484A/F486I lineage and Q493K-alone lineage.

Three of the four escape mutations in the REGN-COV2-treated patient were not identified in Regeneron's viral cell-culture selections (Fig. 2B), illustrating an advantage of complete maps. Viral selections are "incomplete" in the sense that they only identify whatever mutations are stochastically selected in that particular cell-culture experiment. In contrast, complete maps annotate all mutations, which could include mutations that arise for reasons unrelated to treatment but incidentally affect antibody binding.

Of course, viral evolution is shaped by functional constraints as well as pressure to evade antibodies. The mutations selected in cell culture and the patient consistently met the following criteria: they escaped antibody binding, were accessible via a single-nucleotide change, and imposed little or no cost on ACE2 affinity [as measured by prior deep mutational scanning using yeast-displayed RBD (*7*)] (Fig. 2D and fig. S5). Therefore, complete maps of how mutations affect key biochemical phenotypes of the RBD (e.g., ACE and antibody binding) can be used to assess likely paths of viral evolution. A caveat is that over longer evolutionary timeframes, the space of tolerated mutations could shift due to epistatic interactions, as has been observed in viral immune and drug escape (*19*–*21*).

The complete maps enable us to assess what escape mutations are already present among circulating SARS-CoV-2. We examined all human-derived SARS-CoV-2 sequences available as of 11 January 2021, and found a substantial number of RBD mutations that escaped one or more of the antibodies (Fig. 3). However, the only escape mutations present in >0.1% of sequences were the REGN10933 escape-mutant Y453F [0.3% of sequences; see also (*12*)], the REGN10987 escape-mutant N439K [1.7% of sequences; see also Fig. 1C and (*22*)], and the LY-CoV016 escape-mutant K417N (0.1% of sequences; see also Fig. 1C). Y453F is associated with independent outbreaks linked to mink farms in the Netherlands and Denmark (*23*, *24*); notably the mink sequences themselves sometimes also contain other escape mutations such as F486L (*24*). N439K is prevalent in Europe, where it has comprised a large percentage of sequences from regions including Scotland and Ireland (*22*, *25*). K417N is present in the B.1.351 lineage first identified in South Africa (*10*). Another mutation of current interest is N501Y, which is present in B.1.351 and also the B.1.1.7 lineage originally identified in the

United Kingdom (*9*). Our maps indicate that N501Y has no effect on either REGN-COV2 antibody and only a modest effect on LY-CoV016 (Fig. 3).

To determine if the escape maps could be rationalized from the structural interfaces of the antibodies and RBD, we projected the maps onto crystal or cryo-EM structures (Fig. 4A; interactive versions at https://jbloomlab.github.io/SARS-CoV-2-RBD_MAP_clinical_Abs/). As might be expected, escape mutations generally occur in the antibody-RBD interface. However, structures alone are insufficient to predict which mutations mediate escape. For example, LY-CoV016 uses both its heavy and light chains to bind a wide epitope overlapping the ACE2-binding surface, but escape is dominated by mutations at RBD residues that contact the heavy chain CDRs (Fig. 4A and fig. S6, E to G). In contrast, escape from REGN10933 and REGN10987 mostly occurs at RBD residues that pack at the antibody heavy/light-chain interface (Fig. 4A and fig. S6, A to D). The E406W mutation that escapes the REGN-COV2 cocktail occurs at a residue not in contact with either antibody (Fig. 4, A and B). Although E406 is in closer structural proximity to LY-CoV016 (Fig. 4B and fig. S6H), the E406W mutation has a much smaller impact on this antibody (Fig. 1, B and C), suggesting a long-range structural mechanism specific to the REGN-COV2 antibodies (fig. S6I). Taken together, mutations at RBD residues that contact antibody do not always mediate escape, and several prominent escape mutations occur at residues not in contact with antibody (Fig. 4B and fig. S6, D and G).

Overall, we have completely mapped mutations that escape three leading anti-SARS-CoV-2 antibodies. These maps demonstrate that prior characterization of escape mutations was incomplete, identifying neither a single amino-acid mutation that escapes both antibodies in the REGN-COV2 cocktail nor most mutations that arose in a persistently infected patient treated with the cocktail. Of course, our maps still do not answer the most pressing question: will SARS-CoV-2 evolve widespread resistance to these antibodies? But certainly, it is concerning that so many escape mutations impose little cost on RBD folding or receptor affinity, and that some are already present at low levels among circulating viruses. Ultimately, it will be necessary to wait and see what mutations spread as SARS-CoV-2 circulates in the human population. Our work will help with the "seeing," by enabling immediate interpretation of the effects of the mutations cataloged by viral genomic surveillance.

REFERENCES AND NOTES

1. A. Renn, Y. Fu, X. Hu, M. D. Hall, A. Simeonov, Fruitful neutralizing antibody pipeline brings hope to defeat SARS-Cov-2. *Trends Pharmacol. Sci.* **41**, 815–829 (2020). doi:10.1016/j.tips.2020.07.004 Medline
2. M. Caskey, F. Klein, J. C. C. Lorenzi, M. S. Seaman, A. P. West Jr., N. Buckley, G. Kremer, L. Nogueira, M. Braunschweig, J. F. Scheid, J. A. Horwitz, I. Shimeliovich, S. Ben-Avraham, M. Witmer-Pack, M. Platten, C. Lehmann, L. A. Burke, T. Hawthorne, R. J. Gorelick, B. D. Walker, T. Keler, R. M. Gulick, G. Fätkenheuer, S. J. Schlesinger, M. C. Nussenzweig, Viraemia suppressed in HIV-1-infected humans by broadly neutralizing antibody 3BNC117. *Nature* **522**, 487–491 (2015). doi:10.1038/nature14411 Medline
3. J. R. Kugelman, J. Kugelman-Tonos, J. T. Ladner, J. Pettit, C. M. Keeton, E. R. Nagle, K. Y. Garcia, J. W. Froude, A. I. Kuehne, J. H. Kuhn, S. Bavari, L. Zeitlin, J. M. Dye, G. G. Olinger, M. Sanchez-Lockhart, G. F. Palacios, Emergence of Ebola virus escape variants in infected nonhuman primates treated with the MB-003 antibody cocktail. *Cell Rep.* **12**, 2111–2120 (2015). doi:10.1016/j.celrep.2015.08.038 Medline
4. E. A. F. Simões, E. Forleo-Neto, G. P. Geba, M. Kamal, F. Yang, H. Cicirello, M. R. Houghton, R. Rideman, Q. Zhao, S. L. Benvin, A. Hawes, E. D. Fuller, E. Wloga, J. M. N. Pizarro, F. M. Munoz, S. A. Rush, J. S. McLellan, L. Lipsich, N. Stahl, G. D. Yancopoulos, D. M. Weinreich, C. A. Kyratsous, S. Sivapalasingam, Suptavumab for the prevention of medically attended respiratory syncytial virus infection in preterm infants. *Clin. Infect. Dis.* ciaa951 (2020). doi:10.1093/cid/ciaa951 Medline
5. D. Wrapp, N. Wang, K. S. Corbett, J. A. Goldsmith, C.-L. Hsieh, O. Abiona, B. S. Graham, J. S. McLellan, Cryo-EM structure of the 2019-nCoV spike in the prefusion conformation. *Science* **367**, 1260–1263 (2020). doi:10.1126/science.abb2507 Medline
6. A. C. Walls, Y.-J. Park, M. A. Tortorici, A. Wall, A. T. McGuire, D. Veesler, Structure, function, and antigenicity of the sars-CoV-2 spike glycoprotein. *Cell* **181**, 281–292.e6 (2020). doi:10.1016/j.cell.2020.02.058 Medline
7. T. N. Starr, A. J. Greaney, S. K. Hilton, D. Ellis, K. H. D. Crawford, A. S. Dingens, M. J. Navarro, J. E. Bowen, M. A. Tortorici, A. C. Walls, N. P. King, D. Veesler, J. D. Bloom, Deep mutational scanning of SARS-CoV-2 receptor binding domain reveals constraints on folding and ACE2 binding. *Cell* **182**, 1295–1310.e20 (2020). doi:10.1016/j.cell.2020.08.012 Medline
8. A. J. Greaney, T. N. Starr, P. Gilchuk, S. J. Zost, E. Binshtein, A. N. Loes, S. K. Hilton, J. Huddleston, R. Eguia, K. H. D. Crawford, A. S. Dingens, R. S. Nargi, R. E. Sutton, N. Suryadevara, P. W. Rothlauf, Z. Liu, S. P. J. Whelan, R. H. Carnahan, J. E. Crowe Jr., J. D. Bloom, Complete mapping of mutations to the SARS-CoV-2 spike receptor-binding domain that escape antibody recognition. *Cell Host Microbe* **29**, 44–57.e9 (2021). doi:10.1016/j.chom.2020.11.007 Medline
9. A. Rambaut, N. Loman, O. Pybus, W. Barclay, J. Barrett, A. Carabelli, T. Connor, T. Peacock, D. Robertson, E. Volz, "Preliminary genomic characterisation of an emergent SARS-CoV-2 lineage in the UK defined by a novel set of spike mutations," Virological.org (2020); https://virological.org/t/preliminary-genomic-characterisation-of-an-emergent-sars-cov-2-lineage-in-the-uk-defined-by-a-novel-set-of-spike-mutations/563.
10. H. Tegally, E. Wilkinson, M. Giovanetti, A. Iranzadeh, V. Fonseca, J. Giandhari, D. Doolabh, S. Pillay, E. J. San, N. Msomi, K. Mlisana, A. von Gottberg, S. Walaza, M. Allam, A. Ismail, T. Mohale, A. J. Glass, S. Engelbrecht, G. V. Zyl, W. Preiser, F. Petruccione, A. Sigal, D. Hardie, G. Marais, M. Hsiao, S. Korsman, M.-A. Davies, L. Tyers, I. Mudau, D. York, C. Maslo, D. Goedhals, S. Abrahams, O. Laguda-Akingba, A. Alisoltani-Dehkordi, A. Godzik, C. K. Wibmer, B. T. Sewell, J. Lourenço, L. C. J. Alcantara, S. L. K. Pond, S. Weaver, D. Martin, R. J. Lessells, J. N. Bhiman, C. Williamson, T. de Oliveira, Emergence and rapid spread of a new severe acute respiratory syndrome-related coronavirus 2 (SARS-CoV-2) lineage with multiple spike mutations in South Africa. medRxiv 2020.12.21.20248640 [Preprint]. 22 December 2020. https://doi.org/10.1101/2020.12.21.20248640.
11. J. Hansen, A. Baum, K. E. Pascal, V. Russo, S. Giordano, E. Wloga, B. O. Fulton, Y. Yan, K. Koon, K. Patel, K. M. Chung, A. Hermann, E. Ullman, J. Cruz, A. Rafique, T. Huang, J. Fairhurst, C. Libertiny, M. Malbec, W. Y. Lee, R. Welsh, G. Farr, S. Pennington, D. Deshpande, J. Cheng, A. Watty, P. Bouffard, R. Babb, N. Levenkova, C. Chen, B. Zhang, A. Romero Hernandez, K. Saotome, Y. Zhou, M. Franklin, S. Sivapalasingam, D. C. Lye, S. Weston, J. Logue, R. Haupt, M. Frieman, G. Chen, W. Olson, A. J. Murphy, N. Stahl, G. D. Yancopoulos, C. A. Kyratsous, Studies in humanized mice and convalescent humans yield a SARS-CoV-2 antibody cocktail. *Science* **369**, 1010–1014 (2020). doi:10.1126/science.abd0827 Medline
12. A. Baum, B. O. Fulton, E. Wloga, R. Copin, K. E. Pascal, V. Russo, S. Giordano, K. Lanza, N. Negron, M. Ni, Y. Wei, G. S. Atwal, A. J. Murphy, N. Stahl, G. D. Yancopoulos, C. A. Kyratsous, Antibody cocktail to SARS-CoV-2 spike protein prevents rapid mutational escape seen with individual antibodies. *Science* **369**,

1014–1018 (2020). doi:10.1126/science.abd0831 Medline
13. R. Shi, C. Shan, X. Duan, Z. Chen, P. Liu, J. Song, T. Song, X. Bi, C. Han, L. Wu, G. Gao, X. Hu, Y. Zhang, Z. Tong, W. Huang, W. J. Liu, G. Wu, B. Zhang, L. Wang, J. Qi, H. Feng, F.-S. Wang, Q. Wang, G. F. Gao, Z. Yuan, J. Yan, A human neutralizing antibody targets the receptor-binding site of SARS-CoV-2. *Nature* **584**, 120–124 (2020). doi:10.1038/s41586-020-2381-y Medline
14. Regeneron Pharmaceuticals, Inc., "Regeneron's casirivimab and imdevimab antibody cocktail for COVID-19 is first combination therapy to receive FDA emergency use authorization," press release (21 November 2020); https://investor.regeneron.com/news-releases/news-release-details/regenerons-regen-cov2-first-antibody-cocktail-covid-19-receive/.
15. Eli Lilly and Company, "A phase 3 randomized, double-blind, placebo-controlled trial to evaluate the efficacy and safety of LY3819253 alone and in combination with LY3832479 in preventing SARS-CoV-2 infection and COVID-19 in skilled nursing and assisted living facility residents and staff; a NIAID and Lilly Collaborative Study" (Clinical trial registration NCT04497987, clinicaltrials.gov, 2020); https://clinicaltrials.gov/ct2/show/NCT04497987.
16. B. Choi, M. C. Choudhary, J. Regan, J. A. Sparks, R. F. Padera, X. Qiu, I. H. Solomon, H.-H. Kuo, J. Boucau, K. Bowman, U. D. Adhikari, M. L. Winkler, A. A. Mueller, T. Y.-T. Hsu, M. Desjardins, L. R. Baden, B. T. Chan, B. D. Walker, M. Lichterfeld, M. Brigl, D. S. Kwon, S. Kanjilal, E. T. Richardson, A. H. Jonsson, G. Alter, A. K. Barczak, W. P. Hanage, X. G. Yu, G. D. Gaiha, M. S. Seaman, M. Cernadas, J. Z. Li, Persistence and evolution of SARS-CoV-2 in an immunocompromised host. *N. Engl. J. Med.* **383**, 2291–2293 (2020). doi:10.1056/NEJMc2031364 Medline
17. K. S. Xue, T. Stevens-Ayers, A. P. Campbell, J. A. Englund, S. A. Pergam, M. Boeckh, J. D. Bloom, Parallel evolution of influenza across multiple spatiotemporal scales. *eLife* **6**, e26875 (2017). doi:10.7554/eLife.26875 Medline
18. A. F. Feder, S.-Y. Rhee, S. P. Holmes, R. W. Shafer, D. A. Petrov, P. S. Pennings, More effective drugs lead to harder selective sweeps in the evolution of drug resistance in HIV-1. *eLife* **5**, e10670 (2016). doi:10.7554/eLife.10670 Medline
19. J. D. Bloom, L. I. Gong, D. Baltimore, Permissive secondary mutations enable the evolution of influenza oseltamivir resistance. *Science* **328**, 1272–1275 (2010). doi:10.1126/science.1187816 Medline
20. L. I. Gong, M. A. Suchard, J. D. Bloom, Stability-mediated epistasis constrains the evolution of an influenza protein. *eLife* **2**, e00631 (2013). doi:10.7554/eLife.00631 Medline
21. T. H. Zhang, L. Dai, J. P. Barton, Y. Du, Y. Tan, W. Pang, A. K. Chakraborty, J. O. Lloyd-Smith, R. Sun, Predominance of positive epistasis among drug resistance-associated mutations in HIV-1 protease. *PLOS Genet.* **16**, e1009009 (2020). doi:10.1371/journal.pgen.1009009 Medline
22. E. C. Thomson, L. E. Rosen, J. G. Shepherd, R. Spreafico, A. da Silva Filipe, J. A. Wojcechowskyj, C. Davis, L. Piccoli, D. J. Pascall, J. Dillen, S. Lytras, N. Czudnochowski, R. Shah, M. Meury, N. Jesudason, A. De Marco, K. Li, J. Bassi, A. O'Toole, D. Pinto, R. M. Colquhoun, K. Culap, B. Jackson, F. Zatta, A. Rambaut, S. Jaconi, V. B. Sreenu, J. Nix, R. F. Jarrett, M. Beltramello, K. Nomikou, M. Pizzuto, L. Tong, E. Cameroni, N. Johnson, A. Wickenhagen, A. Ceschi, D. Mair, P. Ferrari, K. Smollett, F. Sallusto, S. Carmichael, C. Garzoni, J. Nichols, M. Galli, J. Hughes, A. Riva, A. Ho, M. G. Semple, P. J. M. Openshaw, J. K. Baillie, The ISARIC4C Investigators, the COVID-19 Genomics UK (COG-UK) consortium, S. J. Rihn, S. J. Lycett, H. W. Virgin, A. Telenti, D. Corti, D. L. Robertson, G. Snell, The circulating SARS-CoV-2 spike variant N439K maintains fitness while evading antibody-mediated immunity. bioRxiv 2020.11.04.355842 [Preprint]. 5 November 2020. https://doi.org/10.1101/2020.11.04.355842.
23. European Centre for Disease Prevention and Control, Rapid Risk Assessment: Detection of new SARS-CoV-2 variants related to mink, ECDC, Stockholm, 12 November 2020; www.ecdc.europa.eu/en/publications-data/detection-new-sars-cov-2-variants-mink.
24. B. B. Oude Munnink, R. S. Sikkema, D. F. Nieuwenhuijse, R. J. Molenaar, E. Munger, R. Molenkamp, A. van der Spek, P. Tolsma, A. Rietveld, M. Brouwer, N. Bouwmeester-Vincken, F. Harders, R. Hakze-van der Honing, M. C. A. Wegdam-Blans, R. J. Bouwstra, C. GeurtsvanKessel, A. A. van der Eijk, F. C. Velkers, L. A. M. Smit, A. Stegeman, W. H. M. van der Poel, M. P. G. Koopmans, Transmission of SARS-CoV-2 on mink farms between humans and mink and back to humans. *Science* **371**, 172–177 (2021). doi:10.1126/science.abe5901 Medline
25. A. T. Chen, K. Altschuler, S. H. Zhan, Y. A. Chan, B. E. Deverman, COVID-19 CG: Tracking SARS-CoV-2 mutations by locations and dates of interest. bioRxiv 2020.09.23.310565 [Preprint]. 28 September 2020. https://doi.org/10.1101/2020.09.23.310565.
26. S. Elbe, G. Buckland-Merrett, Data, disease and diplomacy: GISAID's innovative contribution to global health. *Glob. Chall.* **1**, 33–46 (2017). doi:10.1002/gch2.1018 Medline
27. 27. T. Starr, J. Bloom, A. Greaney, A. Addetia, jbloomlab/SARS-CoV-2-RBD_MAP_clinical_Abs: Science revision, Zenodo (2021); https://doi.org/10.5281/zenodo.4443311.
28. W. Hannon, jbloomlab/SARS-CoV-2_chronic-infection-seq: Archived for publication, Version 1, Zenodo (2021); https://doi.org/10.5281/zenodo.4433185.
29. A. E. Wentz, E. V. Shusta, A novel high-throughput screen reveals yeast genes that increase secretion of heterologous proteins. *Appl. Environ. Microbiol.* **73**, 1189–1198 (2007). doi:10.1128/AEM.02427-06 Medline
30. J. Shang, G. Ye, K. Shi, Y. Wan, C. Luo, H. Aihara, Q. Geng, A. Auerbach, F. Li, Structural basis of receptor recognition by SARS-CoV-2. *Nature* **581**, 221–224 (2020). doi:10.1038/s41586-020-2179-y Medline
31. J. Otwinowski, D. M. McCandlish, J. B. Plotkin, Inferring the shape of global epistasis. *Proc. Natl. Acad. Sci. U.S.A.* **115**, E7550–E7558 (2018). doi:10.1073/pnas.1804015115 Medline
32. K. H. D. Crawford, R. Eguia, A. S. Dingens, A. N. Loes, K. D. Malone, C. R. Wolf, H. Y. Chu, M. A. Tortorici, D. Veesler, M. Murphy, D. Pettie, N. P. King, A. B. Balazs, J. D. Bloom, Protocol and reagents for pseudotyping lentiviral particles with SARS-CoV-2 spike protein for neutralization assays. *Viruses* **12**, 513 (2020). doi:10.3390/v12050513 Medline
33. K. H. D. Crawford, A. S. Dingens, R. Eguia, C. R. Wolf, N. Wilcox, J. K. Logue, K. Shuey, A. M. Casto, B. Fiala, S. Wrenn, D. Pettie, N. P. King, A. L. Greninger, H. Y. Chu, J. D. Bloom, Dynamics of neutralizing antibody titers in the months after severe acute respiratory syndrome coronavirus 2 infection. *J. Infect. Dis.* jiaa618 (2020). doi:10.1093/infdis/jiaa618 Medline
34. J. Köster, S. Rahmann, Snakemake—A scalable bioinformatics workflow engine. *Bioinformatics* **28**, 2520–2522 (2012). doi:10.1093/bioinformatics/bts480 Medline
35. S. Chen, Y. Zhou, Y. Chen, J. Gu, fastp: An ultra-fast all-in-one FASTQ preprocessor. *Bioinformatics* **34**, i884–i890 (2018). doi:10.1093/bioinformatics/bty560 Medline
36. H. Li, Aligning sequence reads, clone sequences and assembly contigs with BWA-MEM. arXiv:1303.3997 [q-bio.GN] (26 May 2013).
37. K. Katoh, D. M. Standley, MAFFT multiple sequence alignment software version 7: Improvements in performance and usability. *Mol. Biol. Evol.* **30**, 772–780 (2013). doi:10.1093/molbev/mst010 Medline
38. S. K. Hilton, J. Huddleston, A. Black, K. North, A. S. Dingens, T. Bedford, J. D. Bloom, dms-view: Interactive visualization tool for deep mutational scanning data. *J. Open Source Softw.* **5**, 2353 (2020). doi:10.21105/joss.02353
39. B. J. Grant, A. P. C. Rodrigues, K. M. ElSawy, J. A. McCammon, L. S. D. Caves, Bio3d: An R package for the comparative analysis of protein structures. *Bioinformatics* **22**, 2695–2696 (2006). doi:10.1093/bioinformatics/btl461 Medline

ACKNOWLEDGMENTS

We thank K. Crawford for help with neutralization assays, A. Feder, D. Veesler, N. King, and D. Ellis for helpful comments, and the Fred Hutch Flow Cytometry and Genomics facilities for assistance. **Funding:** This work was supported by the NIAID (R01AI127893 and R01AI141707 to J.D.B. and T32AI083203 to A.J.G.), the Gates Foundation (INV-004949 to J.D.B.), and the Massachusetts Consortium for Pathogen Readiness through grants from the Evergrande Fund (to J.Z.L.). Scientific computing at the Fred Hutch is supported by ORIP grant S10OD028685. T.N.S. is a Washington Research Foundation Innovation Fellow at the University of Washington Institute for Protein Design and an HHMI Fellow of the Damon Runyon Cancer Research Foundation (DRG-2381-19). J.D.B. is an Investigator of the Howard Hughes Medical Institute. **Author contributions:** T.N.S., A.J.G., A.S.D., and J.D.B. designed the study. T.N.S., A.J.G., A.A., and A.S.D. performed the experiments. T.N.S., A.J.G., and J.D.B. analyzed the experimental data. J.Z.L. and M.C.C. sequenced the persistent infection, and

W.W.H. analyzed that data. T.N.S., A.A., W.W.H., and J.D.B. wrote the initial draft, and all authors edited the final version. **Competing interests:** J.Z.L. has consulted for Abbvie and Jan Biotech. The other authors declare no competing interests. **Data and materials availability:** Raw sequencing data are on the NCBI SRA under BioProject PRJNA639956/BioSample SAMN16850904 (escape mapping) and Bioproject PRJNA681234 (patient sequencing). Computer code and processed data for the escape mapping are at (*27*) and https://github.com/jbloomlab/SARS-CoV-2-RBD_MAP_clinical_Abs. Code and data for the patient sequencing are at (*28*) and https://github.com/jbloomlab/SARS-CoV-2_chronic-infection-seq. The sequences of the antibodies are provided via citations in the Material and Methods, the cells and plasmids for the neutralization assays are available in BEI Resources and AddGene (see Materials and Methods for details), and the yeast mutant libraries are available to academic researchers upon request with a completed Materials Transfer Agreement.

SUPPLEMENTARY MATERIALS

science.sciencemag.org/cgi/content/full/science.abf9302/DC1
Materials and Methods
Figs. S1 to S6
References (*29*–*39*)
MDAR Reproducibility Checklist
Data S1

1 December 2020; accepted 19 January 2021
Published online 25 January 2021
10.1126/science.abf9302

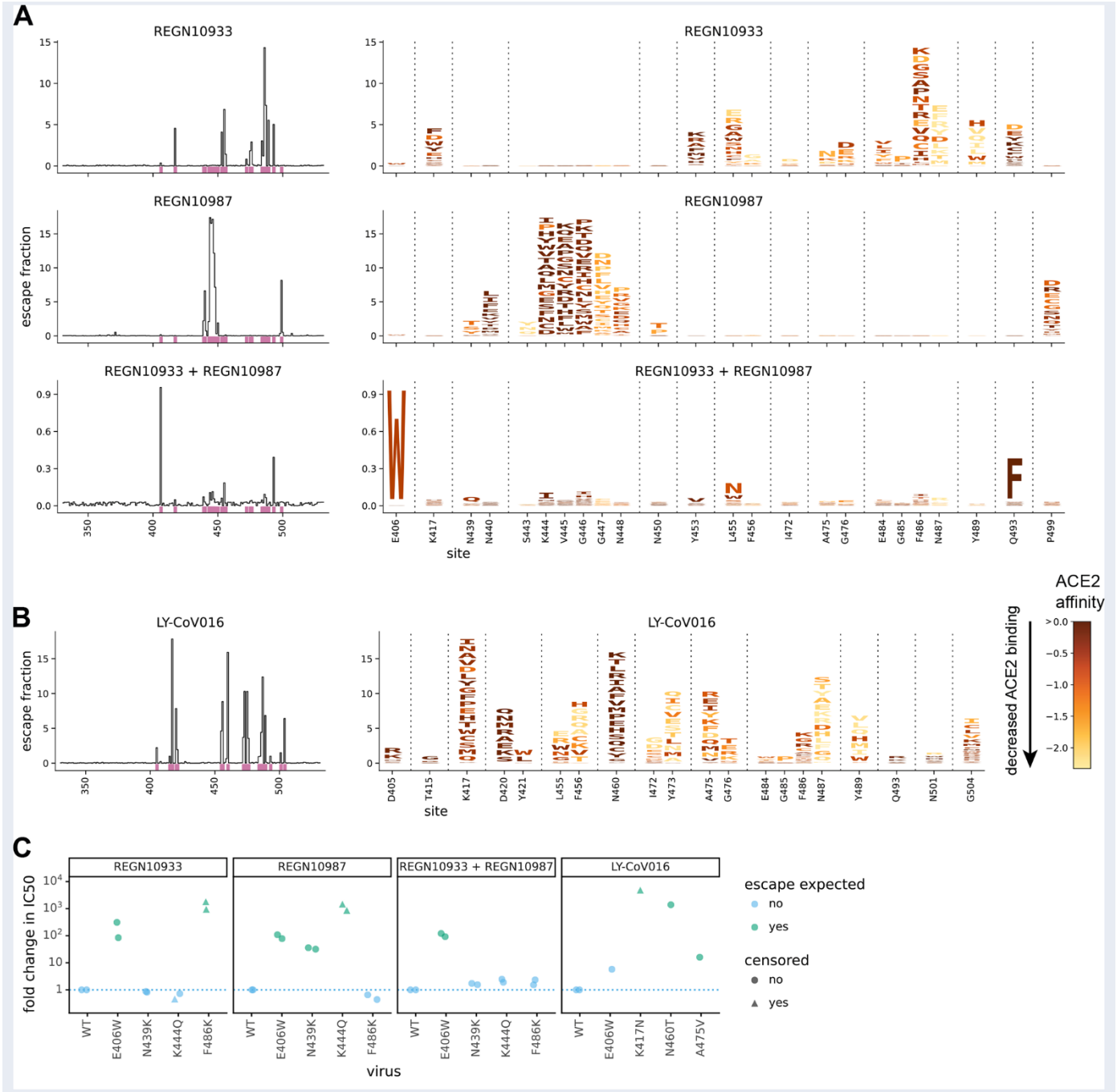

Fig. 1. Complete maps of mutations that escape binding by the REGN-COV2 antibodies and Ly-CoV016. (**A**) Maps for antibodies in REGN-COV2. Line plots at left show escape at each site in the RBD (summed effects of all mutations at each site). Sites of strong escape (purple underlines) are shown in logo plots at right. The height of each letter is proportional to how strongly that amino-acid mutation mediates escape, with a per-mutation "escape fraction" of 1 corresponding to complete escape. The y-axis scale is different for each row, so for instance E406W escapes all REGN antibodies but it is most visible for the cocktail as it is swamped out by other sites of escape for the individual antibodies. See https://jbloomlab.github.io/SARS-CoV-2-RBD_MAP_clinical_Abs/ for zoomable versions. Letters are colored by how mutations affect the RBD's affinity for ACE2 as measured via yeast display (*7*), with yellow indicating poor affinity and brown indicating good affinity; see fig. S2, A and B, for maps colored by how mutations affect expression of folded RBD and fig. S2, C and D, for distribution of effects on ACE2 affinity and RBD expression across all mutations observed among circulating viral isolates. (**B**) Map for LY-CoV016. (**C**) Validation of key mutations in neutralization assays using spike-pseudotyped lentiviral particles. We chose to validate mutations predicted to have large effects or that are present at high frequency among circulating SARS-CoV-2 isolates (e.g., N439K). Each point indicates the fold-increase in inhibitory concentration 50% (IC50) for a mutation relative to the unmutated "wildtype" (WT) spike, which contains D614G. The dotted blue line at 1 indicates wildtype-like neutralization, and values >1 indicate increased neutralization resistance. Point colors indicate if escape was expected at that site from the maps. Point shapes indicate that the fold change is censored (an upper or lower limit) due to the IC50 being outside the dilution series used. Most mutants were tested in duplicate, and so have two points. Full neutralization curves are presented in fig. S3.

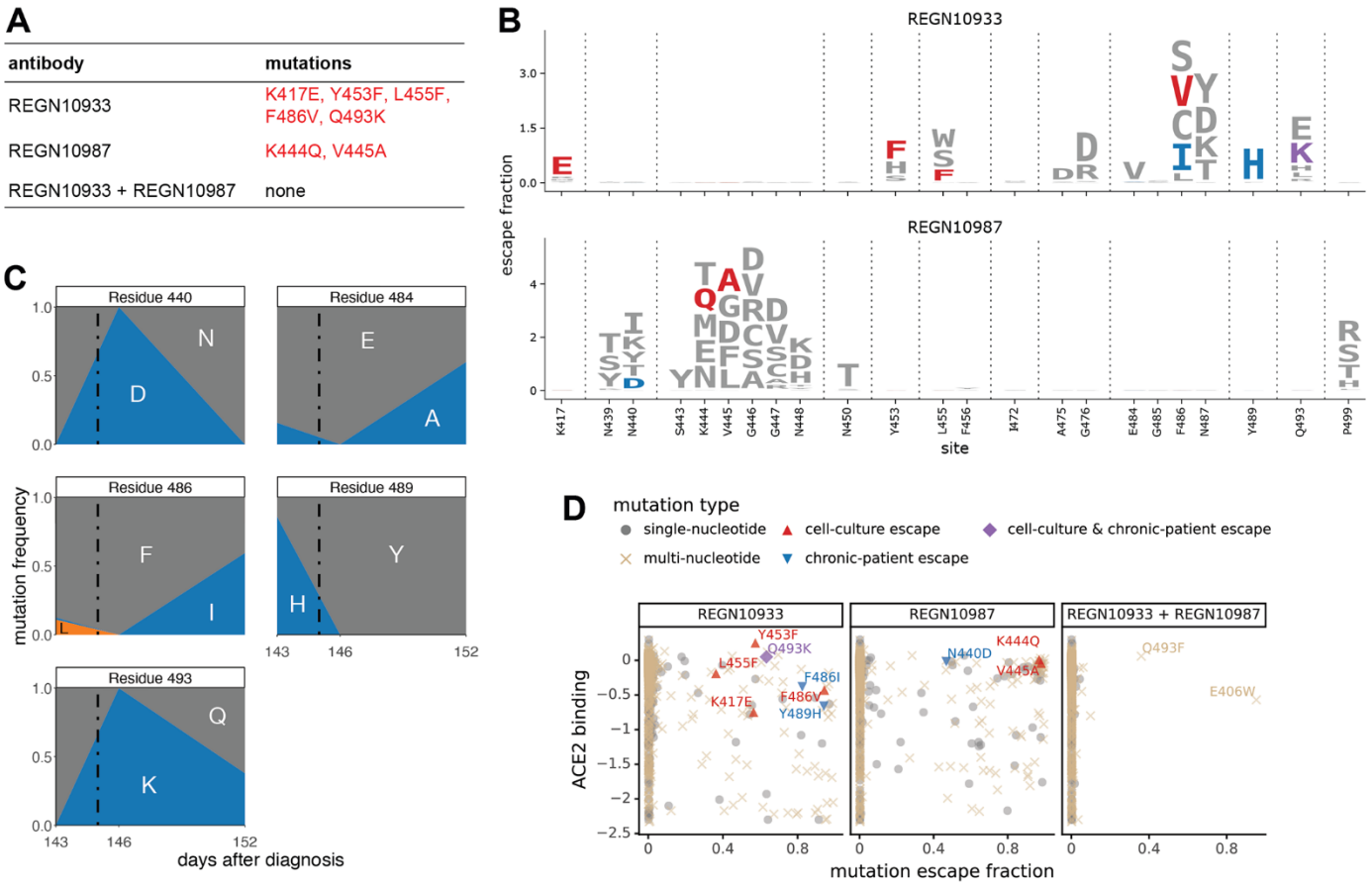

Fig. 2. Escape maps are consistent with viral mutations selected in cell culture and a persistently infected patient. (**A**) Viral escape mutations selected by Regeneron with spike-pseudotyped VSV in cell culture in the presence of antibody (*12*). (**B**) Escape maps like those in Fig. 1A but showing only mutations accessible by single-nucleotide changes to the Wuhan-Hu-1 sequence, with non-gray colors indicating mutations in cell culture (red), in the infected patient (blue), or both (purple). Figure S5 shows these maps colored by how mutations affect ACE2 affinity or RBD expression. (**C**) Dynamics of RBD mutations in a patient treated with REGN-COV2 at day 145 of his infection (black dashed vertical line). E484A rose in frequency in linkage with F486I, but since E484A is not an escape mutation in our maps it is not shown in other panels. See also fig. S4. (**D**) The escape mutations that arise in cell culture and the infected patient are single-nucleotide accessible and escape antibody binding without imposing a large cost on ACE2 affinity [as measured using yeast display (*7*)]. Each point is a mutation with shape/color indicating whether it is accessible and selected during viral growth. Points further to the right on the x-axis indicate stronger escape from antibody binding; points further up on the y-axis indicate higher ACE2 affinity.

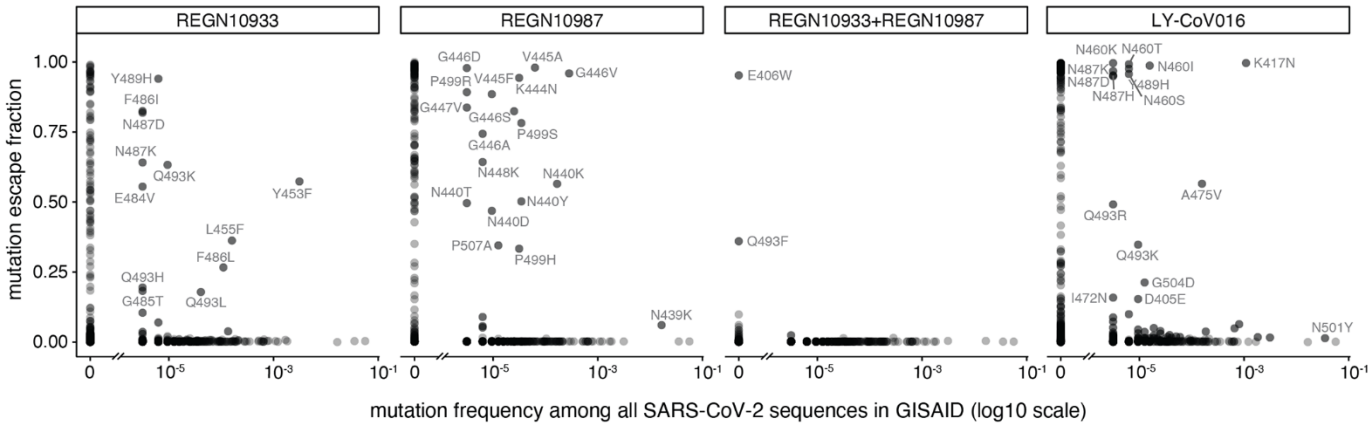

Fig. 3. Antibody escape mutations in circulating SARS-CoV-2. For each antibody or antibody combination, the escape score for each mutation is plotted versus its frequency among the 317,866 high-quality human-derived SARS-CoV-2 sequences on GISAID (*26*) as of January 11, 2021. Escape mutations with notable GISAID frequencies are labeled. The REGN-COV2 cocktail escape mutation E406W requires multiple nucleotide changes from the Wuhan-Hu-1 RBD sequence and is not observed among sequences in GISAID. Other mutations to residue E406 (E406Q and E406D) are observed with low frequency counts, but neither of these mutant amino acids is a single-nucleotide mutation away from W, either.

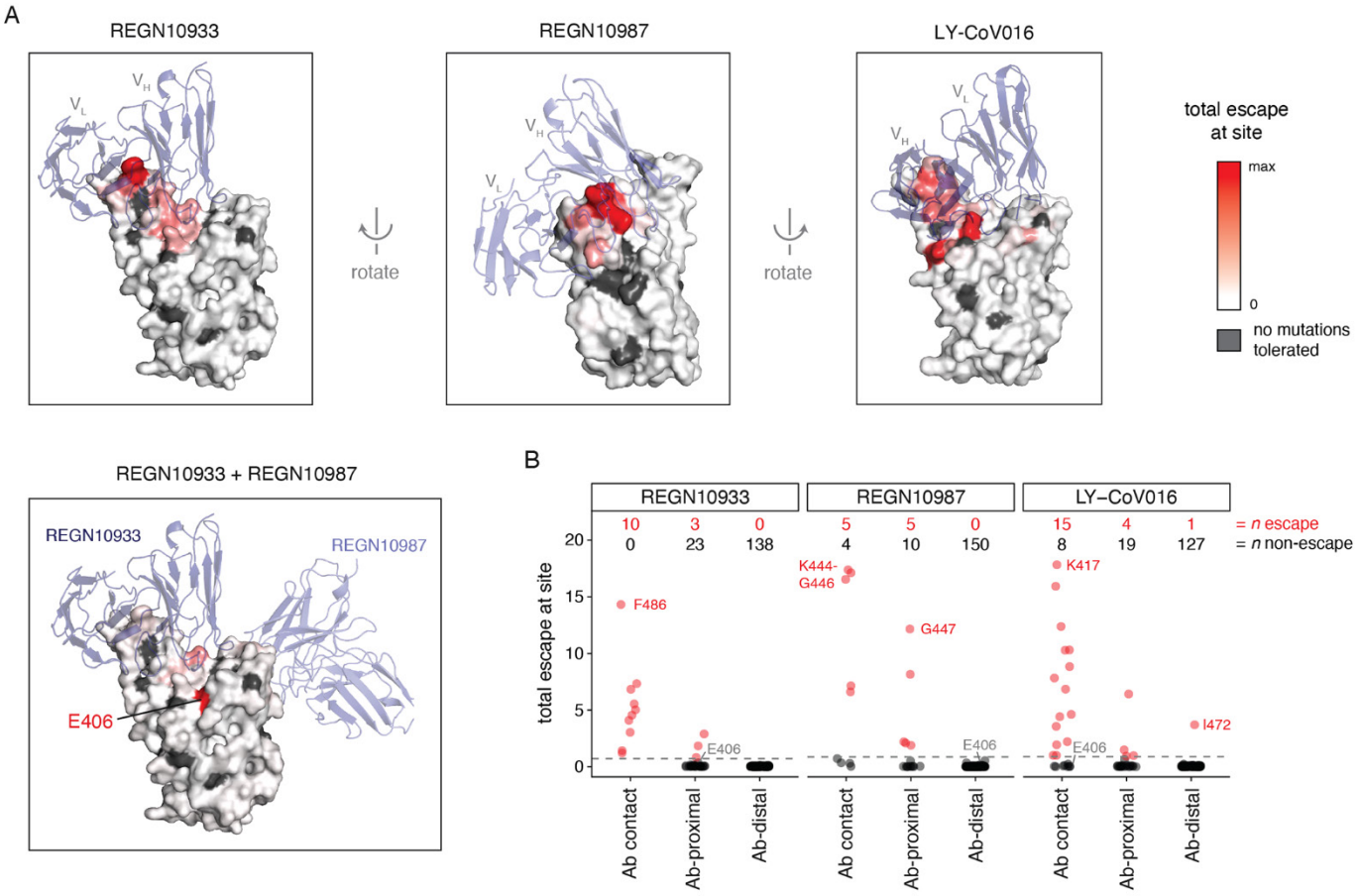

Fig. 4. Structural context of escape mutations. (**A**) Escape maps projected on antibody-bound RBD structures. [REGN10933 and REGN10987: PDB 6XDG (*11*); LY-CoV016: PDB 7C01 (*13*)]. Antibody heavy- and light-chain variable domains are shown as blue cartoons, and the RBD surface is colored to indicate how strongly mutations at that site mediate escape (white indicates no escape, red indicates strongest escape site for that antibody/cocktail). Sites where no mutations are functionally tolerated are colored gray. (**B**) For each antibody, sites were classified as direct antibody contacts (non-hydrogen atoms within 4 Å of antibody), antibody-proximal (4–8 Å), or antibody-distal (>8 Å). Each point indicates a site, classified as escape (red) or non-escape (black). The dashed gray line indicates the cutoff used to classify sites as escape or non-escape (see Methods for details). Red and black numbers indicate how many sites in each category are escape or non-escape sites, respectively. Interactive visualizations are at https://jbloomlab.github.io/SARS-CoV-2-RBD_MAP_clinical_Abs/ and hypothesized mechanisms of escape and additional structural details for labeled points are shown in fig. S6.

Prospective mapping of viral mutations that escape antibodies used to treat COVID-19

Tyler N. Starr, Allison J. Greaney, Amin Addetia, William W. Hannon, Manish C. Choudhary, Adam S. Dingens, Jonathan Z. Li and Jesse D. Bloom

published online January 25, 2021

Science (print ISSN 0036-8075; online ISSN 1095-9203) is published by the American Association for the Advancement of Science, 1200 New York Avenue NW, Washington, DC 20005. The title *Science* is a registered trademark of AAAS.